6-24-2013

Investigation of ripple-limited low-field mobility in large-scale graphene nanoribbons

M. Luisier
Swiss Federal Institute of Technology Zurich

T. B. Boykin
University of Alabama - Huntsville

Z. Ye
University of California - Merced

A. Martini
University of California - Merced

Gerhard Klimeck
Network for Computational Nanotechnology, Birck Nanotechnology Center, Purdue University, gekco@purdue.edu

See next page for additional authors

Luisier, M.; Boykin, T. B.; Ye, Z.; Martini, A.; Klimeck, Gerhard; Kharche, N.; Jiang, X.; and Nayak, S., "Investigation of ripple-limited low-field mobility in large-scale graphene nanoribbons" (2013). *Birck and NCN Publications.* Paper 1424.
http://dx.doi.org/10.1063/1.4811761

AIP | Applied Physics Letters

Investigation of ripple-limited low-field mobility in large-scale graphene nanoribbons

M. Luisier, T. B. Boykin, Z. Ye, A. Martini, G. Klimeck et al.

Citation: Appl. Phys. Lett. **102**, 253506 (2013); doi: 10.1063/1.4811761
View online: http://dx.doi.org/10.1063/1.4811761
View Table of Contents: http://apl.aip.org/resource/1/APPLAB/v102/i25
Published by the AIP Publishing LLC.

Investigation of ripple-limited low-field mobility in large-scale graphene nanoribbons

M. Luisier,[1] T. B. Boykin,[2] Z. Ye,[3] A. Martini,[3] G. Klimeck,[4] N. Kharche,[5] X. Jiang,[6] and S. Nayak[6,7]
[1]*Integrated Systems Laboratory, ETH Zürich, 8092 Zürich, Switzerland*
[2]*Department of ECE, University of Alabama in Huntsville, Huntsville, Alabama 35899, USA*
[3]*School of Engineering, University of California-Merced, Merced, California 95343, USA*
[4]*Network for Computational Nanotechnology, Purdue University, West Lafayette, Indiana 47907, USA*
[5]*Department of Chemistry, Brookhaven National Laboratory, Upton, New York 11973, USA*
[6]*Department of Physics, Rensselaer Polytechnic Institute, Troy, New York 12180, USA*
[7]*School of Basic Sciences, Indian Institute of Technology Bhubaneswar, Bhubaneswar 751013, India*

(Received 13 May 2013; accepted 5 June 2013; published online 26 June 2013)

Combining molecular dynamics and quantum transport simulations, we study the degradation of mobility in graphene nanoribbons caused by substrate-induced ripples. First, the atom coordinates of large-scale structures are relaxed such that surface properties are consistent with those of graphene on a substrate. Then, the electron current and low-field mobility of the resulting non-flat nanoribbons are calculated within the Non-equilibrium Green's Function formalism in the coherent transport limit. An accurate tight-binding basis coupling the σ- and π-bands of graphene is used for this purpose. It is found that the presence of ripples decreases the mobility of graphene nanoribbons on SiO_2 below 3000 cm^2/Vs, which is comparable to experimentally reported values.
 [http://dx.doi.org/10.1063/1.4811761]

The amazing electrical[1] and thermal[2] characteristics of graphene make it an attractive candidate as a future logic component in digital and analog circuits.[3,4] In such applications, excellent electron and hole transport properties are required, which is fulfilled by graphene,[5] but at the expense of the band gap. The absence of the band gap does not allow one to properly switch off transistors in stand-by mode due to the presence of high source-to-drain tunneling rates. To circumvent this energy loss problem and to enhance the device performance, graphene can be patterned into quasi 1-D nanoribbons with geometry-tunable band gaps.[6,7]

Hence, graphene nanoribbons (GNRs) might become a credible alternative to Si-based field-effect transistors (FETs) in post complementary metal-oxide-semiconductor (CMOS) circuits. However, due to their reduced lateral dimensions, they are more prone to scattering than 2-D graphene sheets and have therefore significantly lower carrier mobilities.[8] To improve the transport properties of GNRs, it is essential to identify all their major sources of scattering, for example, through numerical simulations so that they can be minimized. This is the goal of this study. While line edge roughness, defects, acoustic, optical, and remote phonon scattering are known to affect the behavior of graphene nanoribbons, very little attention has been paid to ripples or surface corrugations and their influence on mobility.

As demonstrated in Ref. 9 for SiO_2 and Ref. 10 for boron nitride (BN), graphene conforms to the underlying substrate. If the substrate surface is not flat, the graphene layer deposited on it exhibits wave patterns, as shown in Fig. 1(a). The distribution of these ripples is not completely random: based on experimental measurements (scanning probe microscopy), a correlation function $g(r)$ can usually be defined to characterize the height $z(x, y)$ of the carbon atoms above a reference plane.[9] Note that r represents the distance between two atoms. Two important quantities can be extracted from $g(r)$, the root mean square Δ_{rms}, and the correlation length L_c of the atom height. If both are known, it is possible to numerically construct realistic graphene surfaces that can be used as input to mobility calculations.

Ripples modify not only the atomic structure of graphene but also its chemical bond interactions. In a flat monolayer, two distinct sets of orbitals can be identified, one including the orbitals connected through σ-bonds (e.g., s, p_x, p_y, $\cdots$) and one for the orbitals connected through π-bonds (e.g., p_z, d_{yz}, d_{zx}, $\cdots$). Since the two groups do not interact with each other, they can be treated separately. However, when some atoms are moved out of the reference plane, they start to couple to each other through σ- and π-bonds, as illustrated in Fig. 2. For example, s and p_z orbitals, which do not overlap in a flat graphene sheet, are connected through σ-bonds in case of ripples. Similarly, σ- and π-bonds couple p_x and p_z orbitals in non-flat structures.

Based on these observations, it is clear that the single-p_z orbital model, although widely used to simulate graphene devices,[12] cannot estimate ripple-limited mobilities. In fact, the p_z model is inaccurate even when restricted to modeling only the π-bands of perfectly flat bulk graphene or armchair nanoribbons (AGNRs). It also permits no realistic hydrogen passivation model. These glaring defects led us to increase the basis set for the π-bands by adding d_{yz} and d_{zx} orbitals, along with a realistic hydrogen passivation approach, resulting in accurate bands for both bulk graphene and hydrogen-passivated AGNRs.[13]

Similarly, only an extension of the basis set can account for the coupling of the σ- and π-bands of graphene induced by ripples. This is why we have recently developed an sp^3d^5 nearest-neighbor (no spin-orbit) tight-binding model[14] specifically dedicated to arbitrary bulk graphene, nanoribbons,

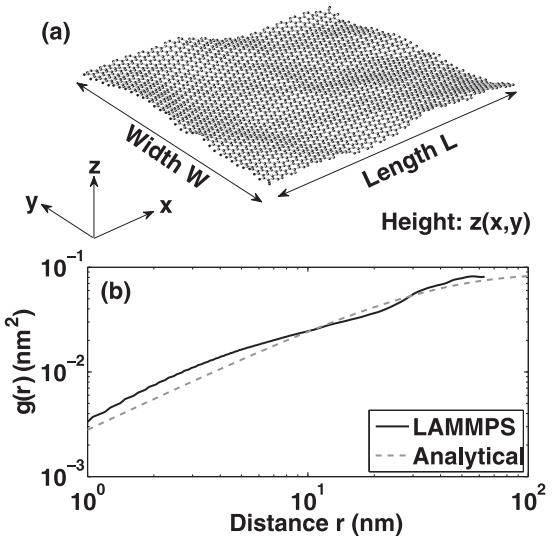

FIG. 1. (a) Schematic view of a graphene nanoribbon of length L (along the x-axis) and width W (along y) including substrate-induced ripples (along z). (b) Height-height correlation function $g(r) = \langle (z(x+r,y) - z(x,y))^2 \rangle$ extracted from the atom coordinates generated by molecular dynamics simulations (solid line) and calculated analytically assuming an exponential autocovariance function for the height $z(x, y)$ of the carbon atoms above a flat reference plane (dashed line). The quantities Δ_{rms} and L_c indicate the root mean square and correlation length of the height $z(x, y)$, respectively. Here, $\Delta_{rms} = 0.19$ nm and $L_c = 30$ nm as in Ref. 9.

and multi-layer structures. Because d-orbitals are needed for even the π-bands of perfectly flat graphene, the full set of d-orbitals is explicitly considered. Other approaches that consider d-orbitals do not include them explicitly, but only their lowest-order effects on the s-and p-orbitals via perturbation theory.[15] Strain is included through a modification of Harrison's rule.[16] The bulk and strain parameters of the sp^3d^5 tight-binding model are fit to density-functional theory (DFT) calculations, achieving very good agreement, but at a far lower computational cost. Hence, the expanded model is integrated into a full-band, atomistic quantum transport solver based on the Non-equilibrium Green's Function (NEGF) formalism[17] to allow for fast and accurate simulations of graphene structures and their ripple-limited low-field mobility $\mu_{ripples}$.

Molecular dynamics (MD) simulations are performed using LAMMPS software[11] to construct graphene sheets having

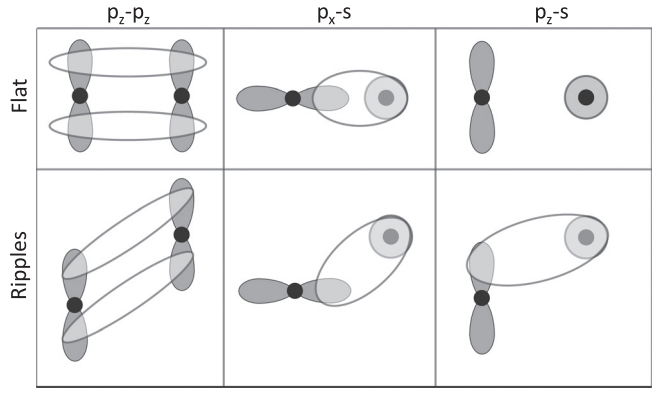

FIG. 2. Illustration of the bond coupling between two p_z (left), a p_x and s (center), and a p_z and s orbital (right) in a flat (up) and non-flat (bottom) graphene nanoribbon. Ripples induce additional σ- and/or π-coupling between orbital sets that do not interact with each other in flat structures: (s, p_x, p_y, d_{xy}, $d_{x^2-y^2}$, $d_{3z^2-r^2}$) and (p_z, d_{yz}, d_{zx}).

rippled surfaces characterized by a height-height correlation function with experimentally realistic values of root mean square, Δ_{rms}, and correlation length, L_c. An Adaptive Intermolecular Reactive Empirical Bond Order (AIREBO) potential[18] is used to describe the interactions between the carbon atoms. Time steps of 0.002 ps and a Langevin thermostat are applied to the free atoms in the system to maintain a temperature of 300 K. First, the fixed ends of perfectly flat structures are displaced along the length direction towards each other (displacement of ~0.96 nm). Then the resulting system is allowed to relax for a minimum of 40 000 time steps. When the desired Δ_{rms} and L_c are reached, the MD simulations are stopped.

For graphene on SiO_2 substrates, Δ_{rms} and L_c are 0.19 and 30 nm, respectively.[9] Nanoribbons with dimensions much smaller than the ripple correlation length cannot be constructed with LAMMPS and exhibit the right Δ_{rms} and L_c. For this reason, large-scale GNRs must be considered. In this work, their length L is set to 120 nm and their width W to 20.5 nm. Such structures contain 97 440 atoms corresponding to Hamiltonian matrices of size 876 960 in the sp^3d^5 tight-binding model. The height-height correlation function $g_{LAMMPS}(r)$ of one nanoribbon sample created by LAMMPS is reported in Fig. 1(b). To demonstrate that the values of Δ_{rms} and L_c for this sample are correct, $g_{LAMMPS}(r)$ is compared to its experimentally determined analytic form[9]

$$g_{analytical}(r) = 2\Delta_{rms}^2(1 - \exp(-r/L_c)). \tag{1}$$

A good agreement between $g_{LAMMPS}(r)$ and $g_{analytical}(r)$ can be observed in Fig. 1(b), where an exponential autocovariance function is assumed for the atom height $z(x, y)$ in Eq. (1).

To calculate the ripple-limited low-field mobility of the graphene nanoribbons generated by LAMMPS, their energy-resolved transmission probability $T(E)$ and total density-of-states $D(E, x, y)$ are first computed within the NEGF formalism expressed in our sp^3d^5 tight-binding basis and in the coherent transport limit, without solving the Poisson equation. The mean transmission value averaged over 20 GNR samples with different ripple configurations, its maximum and minimum values, as well as the transmission through a flat structure are shown in Fig. 3(a). From $T(E)$ and $D(E, x, y)$, the electron current I_d and charge density n_d can be evaluated for each sample using

$$I_d = -\frac{2e}{\hbar}\int \frac{dE}{2\pi} T(E)\left(-\frac{df(E,E_F)}{dE}\right) e\Delta V, \tag{2}$$

$$n_d = \frac{2}{L}\int dxdy \int dE\, D(E,x,y) f(E,E_F), \tag{3}$$

where the factor 2 stands for the two spin contributions, e is the elementary charge, $\hbar$ the reduced Planck's constant, $L = 120$ nm the GNR length, ΔV the small bias applied between its two ends, E_F the electron Fermi level, and $f(E, E_F)$ the Fermi distribution function.

The charge density of rippled graphene nanoribbons varies quite rapidly along the x- and y-axis due to the non-uniformity of the density-of-states. As a consequence, the mobility becomes position-dependent. However, since a

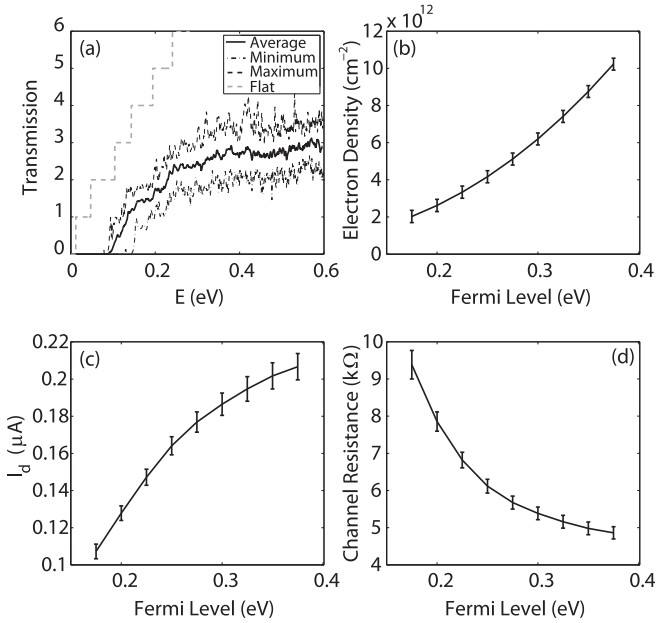

FIG. 3. (a) Energy-resolved transmission probability through a graphene nanoribbon with $L = 120$ nm and $W = 20.5$ nm. The solid line refers to the mean transmission averaged over 20 samples when ripples are included ($\Delta_{rms} = 0.19$ nm, $L_c = 30$ nm), the thin dashed (dashed-dotted) line to the maximum (minimum) value of the transmission, and the dashed gray line to the transmission through a flat nanoribbon. (b) Mean electron density in the channel of the same graphene nanoribbon as in (a) as a function of the Fermi level position at room temperature. A bias difference $\Delta V = 1$ mV is applied between the two ends of the structure. The error bars indicate the standard deviation from the mean values. (c) Same as (b), but for the electron current I_d. (d) Same as (b) and (c), but for the channel resistance $R = \Delta V / I_d$.

single mean mobility is usually extracted from experimental devices, the charge density in Eq. (3) is averaged over x and y to smooth its spatial variations. It is therefore important to realize that, locally, the mobility might be larger or smaller than what is reported.

The mean value of the charge density $n_{d,mean}$, electron current $I_{d,mean}$, and channel resistance $R_{d,mean} = \Delta V / I_{d,mean}$ averaged over 20 samples are reported in Figs. 3(b)–3(d) as a function of the Fermi level E_F. Considering only 20 GNR samples is justified by the fact that n_d, I_d, and R_d do not present large statistical variations from one sample to the other, as indicated by the error bars in Fig. 3.

The last simulation step consists in extracting $\mu_{ripples}$ from n_d and R_d. This is achieved by solving the following equation:

$$\mu_{ripples} = \left(\frac{R_d - R_0}{L} \right)^{-1} \frac{1}{e n_d}. \quad (4)$$

The ballistic resistance R_0 is calculated based on the transmission probability through a flat nanoribbon, as shown in Fig. 3(a). Equation (4) is similar to the "dR/dL" method,[19] which requires diffusive electron transport and therefore no localization effects. Since no isolated peak emerges from the transmission curves in Fig. 3(a), it can be concluded that there are no strong localization effects and transport is mainly diffusive.

The room temperature, ripple-limited mobility of large-scale graphene nanoribbons on SiO_2 is plotted in Fig. 4 as a function of the charge density n_d. As can be seen, ripples and

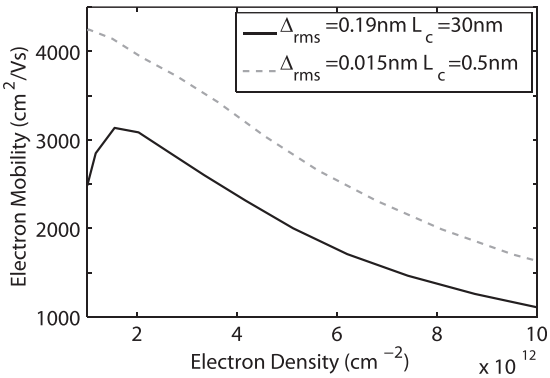

FIG. 4. Ripple-limited low-field mobility in a graphene nanoribbon with $L = 120$ nm and $W = 20.5$ nm at room temperature. Two cases are plotted: ($\Delta_{rms} = 0.19$ nm, $L_c = 30$ nm), which corresponds to the data of SiO_2 substrates as in Ref. 9 and ($\Delta_{rms} = 0.015$ nm, $L_c = 0.5$ nm), where the root mean square of BN substrates is used as in Ref. 10 (no experimental L_c value known).

corrugations have a large influence on the mobility, which barely exceeds 3000 cm^2/Vs, even at low carrier densities. The ripple-limited mobility is about one order of magnitude smaller than the one originating from line edge roughness or electron-phonon scattering,[8] indicating the critical influence of the structural spatial variations of ripples on the device performance. The resulting low mobility values correspond well to the experimental data reported in Ref. 20, both in terms of magnitude and shape (maximum mobility at a carrier concentration around 2×10^{12} cm^{-2}).

As a second example, BN substrates are considered. While the root mean square of the BN surface has been well established, $0.01 \leq \Delta_{rms} \leq 0.02$ nm,[10] the correlation length is unknown. As a solution to this problem, we have set $\Delta_{rms} = 0.015$ nm and let LAMMPS automatically determine L_c. The resulting value is 0.5 nm, but its accuracy is uncertain. For this reason, these substrates are more properly viewed as pseudo-BN instead of actual BN. Following the procedure for SiO_2 substrates, a ripple-limited mobility is extracted for graphene on pseudo-BN and is shown in Fig. 4. A 30% increase can be observed compared to SiO_2, which is less than the benefit expected from real BN substrates.[21] These relatively low mobility values for graphene on pseudo-BN are most likely due to the short correlation length predicted by LAMMPS. Further investigations are needed to better mimic real BN substrates.

In conclusion, we have developed a simulation approach based on molecular dynamics and quantum transport to study the ripple-limited mobility component of large-scale graphene nanoribbons deposited on SiO_2. Values below $\sim$3000 cm^2/Vs have been found at low and high charge densities. This indicates that the morphology of the underlying substrate surface strongly limits the maximum achievable mobility of graphene. It remains to be determined how ripples with a large correlation length may impact ultra-narrow graphene nanoribbons. If the atom height does not vary much along the width direction, ripples may have a small influence on the total mobility, which will be dominated by line edge roughness.

This work was supported by SNF grant (No. PP00P2_133591), by a grant from the Swiss National

Supercomputing Centre (CSCS) under project ID s363, by NSF grant (No. EEC-0228390) that funds the Network for Computational Nanotechnology, by NSF PetaApps grant (No. 0749140), and by NSF through XSEDE resources provided by the National Institute for Computational Sciences (NICS).

[1]X. Du, I. Skachko, A. Barker, and E. Y. Andrei, Nat. Nanotechnol. **3**, 491 (2008).
[2]J. H. Seol, I. Jo, A. L. Moore, L. Lindsay, Z. H. Aitken, M. T. Pettes, X. S. Li, Z. Yao, R. Huang, D. Broido, N. Mingo, R. S. Ruoff, and L. Shi, Science **328**, 213 (2010).
[3]Y. Wu, Y.-M. Lin, A. A. Bol, K. A. Jenkins, F. Xia, D. B. Farmer, Y. Zhu, and P. Avouris, Nature (London) **472**, 74 (2011).
[4]Y.-M. Lin, A. Valdes-Garcia, S.-J. Han, D. B. Farmer, I. Meric, Y. Sun, Y. Wu, C. Dimitrakopoulos, A. Grill, P. Avouris, and K. A. Jenkins, Science **332**, 1294 (2011).
[5]J.-H. Chen, C. Jang, S. Xiao, M. Ishigami, and M. S. Fuhrer, Nat. Nanotechnol. **3**, 206 (2008).
[6]M. Y. Han, B. Ozyilmaz, Y. Zhang, and P. Kim, Phys. Rev. Lett. **98**, 206805 (2007).
[7]X. Li, X. Wang, L. Zhang, S. Lee, and H. Dai, Science **319**, 1229 (2008).
[8]T. Fang, A. Konar, H. Xing, and D. Jena, Phys. Rev. B **78**, 205403 (2008).
[9]M. Ishigami, J. H. Chen, W. G. Cullen, M. S. Fuhrer, and E. D. Williams, Nano Lett. **7**, 1643 (2007).
[10]R. Decker, Y. Wang, V. W. Brar, W. Regan, H.-Z. Tsai, Q. Wu, W. Gannett, A. Zettl, and M. F. Crommie, Nano Lett. **11**, 2291 (2011).
[11]S. J. Plimpton, J. Comp. Phys. **117**, 1 (1995).
[12]G. Fiori and G. Iannaccone, IEEE Electron Devices Lett. **28**, 760 (2007).
[13]T. B. Boykin, M. Luisier, G. Klimeck, X. Jiang, N. Kharche, and S. K. Nayak, J. Appl. Phys. **109**, 104304 (2011).
[14]T. B. Boykin, M. Luisier, N. Kharche, X. Jaing, S. K. Nayak, A. Martini, and G. Klimeck, in *2012 15th International Workshop on Computational Electronics (IWCE), May 2012*.
[15]S. Konschuh, M. Gmitra, and J. Fabian, Phys. Rev. B **82**, 245412 (2010).
[16]W. A. Harrison, *Elementary Electronic Structure* (World Scientific, 1999).
[17]M. Luisier, A. Schenk, W. Fichtner, and G. Klimeck, Phys. Rev. B **74**, 205323 (2006).
[18]S. J. Stuart, A. B. Tutein, and J. A. Harrison, J. Chem. Phys. **112**, 6472 (2000).
[19]K. Rim, S. Narasimha, M. Longstreet, A. Mocuta, and J. Cai, IEDM Tech. Dig. **2002**, 43.
[20]V. E. Dorgan, M.-H. Bae, and E. Pop, Appl. Phys. Lett. **97**, 082112 (2010).
[21]C. R. Dean, A. F. Young, I. Meric, C. Lee, L. Wang, S. Sorgenfrei, K. Watanabe, T. Taniguchi, P. Kim, K. L. Shepard, and J. Hone, Nat. Nanotechnol. **5**, 722 (2010).